Granular Matter 6, 167–172 © Springer-Verlag 2004
DOI 10.1007/s10035-004-0161-2

Numerical simulation of particle motion in dense phase pneumatic conveying

Jiansheng Xiang, Don McGlinchey

Abstract A gas-solids two-dimensional mathematical model was developed for plug flow of cohesionless particles in a horizontal pipeline in dense phase pneumatic conveying. The model was developed based on the discrete element method (DEM). For the gas phase, the Navier-Stokes equations were integrated by the semi-implicit method for pressure-linked equations (SIMPLE) scheme of Patankar employing the staggered grid system. For the particle motion the Newtonian equations of motion of individual particles were integrated, where repulsive and damping forces for particle collision, the gravity force, and the drag force were taken into account. For particle contact, a nonlinear spring and dash pot model for both normal and tangential components was used. In order to get more realistic results, the model uses realistic pneumatic system and material values.

Keywords Pneumatic conveying, Plug flow

1 Introduction

Dense phase pneumatic transport of bulk materials has become an important technology in many industries: from pharmaceuticals to petro-chemicals and power generation. This is due to the increasing demands for product quality, and of environmental legislation. Much current industrial interest centers on a particular mode of dense phase transport called 'plug flow'. This type of low velocity pneumatic conveying has been quoted as causing less particle attrition, reduced component wear, and lower energy costs. For these reasons, plug flow systems are widely applied in many modern industrial applications. [1]

The discrete element method (DEM), sometimes called the distinct element method, is becoming widely used in simulating granular flows. Pioneering work in the application of the method to granular systems was carried out by Cundall and Strack(1979) [2]. Also they developed the program BALL to simulate assemblies of discs. Early work concentrated on the use of 'springs and dashpots' to represent particle interactions.

Y.Tsuji [3] [4] further developed and modified Cundall and Strack's model, where DEM was first employed in simulation of a plug flow system. The Ergun equation was applied to give the fluid force acting on particles in a moving or stationary bed. The wave-like motion of the flow boundary was observed clearly in that simulation. And good agreement was obtained for the relation between the height of the stationary deposited layer and the plug flow velocity. But due to the limitation of computation time, the author only considered the large particles ($d > 10\,\mathrm{mm}$), and simulated a short pipe with only 1000 particles. Quantitative disagreement was observed in the results.

To make the calculation to be more realistic, the present authors consider smaller particles (d=3 mm), longer pipe (L=8 m) and simulate more than 40000 particles. A nonlinear spring and dashpot model has been employed in the present work combined with finite difference method and SIMPLE method (Semi-Implicit Method for Pressure-Linked Equation).

Received: 22 July 2003

J. Xiang (✉)
Institute of Particle Science and Engineering,
School of Process, Environmental and Materials Engineering,
University of Leeds,
Leeds, LS2 9JT, UK
e-mail: j.xiang@leeds.ac.uk
Tel.: +44 (0)113 343 2357
Fax: +44 (0)113 343 2405

D. McGlinchey
School of Engineering,
Science and Design,
Glasgow Caledonian University,
Cowcaddens Road, Glasgow, G4 OBA, UK
e-mail: d.mcglinchey@gcal.ac.uk
Tel.: 44 (0)141 331 3713
Fax: 44 (0)141 331 3448

2 Model

2.1 The Equation of Motion of Particles

Let's take individual particles into consideration. In pneumatic conveying systems, individual particles have two types of motion, translational and rotational. The motions of particles are influenced by the gravitational force, contact forces of particle-particle and particle-wall, and fluid drag forces.

According to Newton's second law of motion the differential equation of particle motion can be written as:

$$\sum \mathbf{F} = m\ddot{\mathbf{x}} = \mathbf{F_D} + \mathbf{F_C} + m\mathbf{g} \tag{1}$$

$$\sum \mathbf{M} = I_m \ddot{\boldsymbol{\theta}} \tag{2}$$

where $\ddot{\mathbf{x}}$ and $\ddot{\boldsymbol{\theta}}$ are the acceleration and angle acceleration of the particle, $\mathbf{M}$ and $\mathbf{F}$ are the total forces and torque caused by contact acting on the particle, $\mathbf{F_D}$ is the fluid drag force, $\mathbf{F_C}$ is the total contact force, $\mathbf{g}$ is the gravity acceleration vector.

The positions and the velocities are calculated as follows,

$$\dot{\mathbf{x}}(t+\Delta t) = \dot{\mathbf{x}}(t) + \ddot{\mathbf{x}}\Delta t \tag{3a}$$

$$\mathbf{x}(t+\Delta t) = \mathbf{x}(t) + \dot{\mathbf{x}}\Delta t \tag{3b}$$

$$\dot{\boldsymbol{\theta}}(t+\Delta t) = \dot{\boldsymbol{\theta}}(t) + \ddot{\boldsymbol{\theta}}\Delta t \tag{3c}$$

$$\boldsymbol{\theta}(t+\Delta t) = \boldsymbol{\theta}(t) + \dot{\boldsymbol{\theta}}\Delta t \tag{3d}$$

where $\dot{\mathbf{x}}$ and $\mathbf{x}$ are velocity and displacement of the particle, $\boldsymbol{\theta}$ and $\dot{\boldsymbol{\theta}}$ are angle and angular velocity of the particle.

2.2 Contact Force

A review of the literature reveals that the contact models describing the force-displacement relationships range from simple linear spring, dash-pot model to nonlinear spring, dash-pot models. Zhang and Whiten [5] have shown that the nonlinear contact force model was found to give more realistic results. In the present work, this model is employed.

In calculating contact forces, the contact of particles is modeled by a pair of spring-dashpot in both the normal and tangential directions. In the tangential direction, the maximum static force is involved in the calculation.

$$\mathbf{F_{nij}} = \left(-k_n \delta_{nij}^{3/2} - \eta_n \mathbf{U_{rij}} \mathbf{n}_{ij}\right) \mathbf{n}_{ij} \tag{4a}$$

$$\mathbf{F_{tij}} = \min\left\{-k_t \delta_{\mathbf{tij}} - \eta_n \mathbf{U_{sij}}, -\mu_f \left|\mathbf{F_{nij}}\right| \mathbf{t_{ij}}\right\} \tag{4b}$$

where δ_{nij},δ_{tij} are normal and tangential displacements, $\mathbf{U_{rij}}$ is the relative velocity of Particle i to Particle j, $\mathbf{n_{ij}}$ is the unit vector from the center of Particle i to Particle j, $\mathbf{U_{sij}}$ is the slip velocity of contact point, $\mathbf{t_{ij}}$ is the unit vector perpendicular with $\mathbf{n_{ij}}$.

2.2.1 Force-Displacement Law

According to the Hertzian contact theory, the relation between the normal force $\mathrm{F_n}$ and displacement δ_{n} is given by,

$$F_n = K_n \delta_n^{3/2} \tag{5}$$

For two different spheres, $\mathrm{K_n}$ is given below,

$$K_n = \frac{4\sqrt{r^*}/3}{(1-\sigma_1^2)/E_1 + (1-\sigma_2^2)/E_2}$$

$$r^* = \frac{r_1 r_2}{r_1 + r_2} \tag{6}$$

where E is the Young's modulus, σ is the Poisson ratio of the particles, r is the radius of particles.

The relation between the tangential force $\mathrm{F_t}$ and displacement δ_{t} was derived by Mindlin and Deresiewicz. [8]

$$F_t = K_t \delta_t \tag{7}$$

$$K_t = \frac{8\sqrt{r^*}\delta_n^{1/2}}{(2-\sigma_1)/G_1 + (2-\sigma_2)/G_2} \tag{8}$$

$$r^* = \frac{r_1 r_2}{r_1 + r_2}$$

$$G_1 = \frac{E_1}{2(1+\sigma_1)}$$

$$G_2 = \frac{E_2}{2(1+\sigma_2)}$$

2.2.2 Damping coefficient

In the present work, Tsuji's model of the damping coefficient has been employed. The damping coefficient η_{n} is shown below,

$$\eta_n = \alpha \left(m K_n\right)^{1/2} \delta_n^{1/4} \tag{9}$$

$$m = \frac{m_1 m_2}{m_1 + m_2}$$

where η_{n} is the damping coefficient in the normal direction,

The damping coefficient η_{t} in the tangential direction is assumed to be equal to η_{n} in this work.

To save the computational time, the methods for searching contact coupling particles, neighborhood list and boxing, are employed in present model.

2.3 Drag force

In the present work, the finite difference method is used. The flow domain is divided into cells, the cell size is 16 mm*16 mm. The continuity equation is shown below,

For Gas phase:

$$\frac{\partial(\rho_g \varepsilon_g \mathbf{u})}{\partial t} + \nabla \cdot (\rho_g \varepsilon_g \mathbf{u}\mathbf{u}) = \nabla \cdot (\mu_g \varepsilon_g \nabla(\mathbf{u})) - \varepsilon_g \nabla p - F_{t,D} + \varepsilon_g \rho_{\mathrm{g}} \mathbf{g} \tag{10}$$

where ρ_{g} is the fluid density, ε_g is the fluid voidage, p is the pressure, μ_{g} dynamic fluid viscosity, $\mathrm{F_{t,D}}$ is total drag force acting on gas phase.

As implied in equation (1), the fluid drag force should be determined on an individual particle basis. But it is difficult to calculate this force theoretically. Correlations have been developed by Ergun equation [6] and Wen-Yu [7]. For individual particles, the drag force acting on a single particle is derived from these correlations.

Since the model is two-dimensional, the length of cell in Z-direction is equal to the diamenter of the particles, the value of fluid voidage is bigger than in a three-dimensional model. The drag force calculated by Ergun equation and Wen-Yu correlation is influenced by the value of the voidage. Therefore, the voidage is modified by a coefficient $\mathrm{C_V}$ that is calculated by comparing the value of voidage between model and experimentation.

$$\varepsilon_g' = C_\nu \varepsilon_g \tag{11}$$

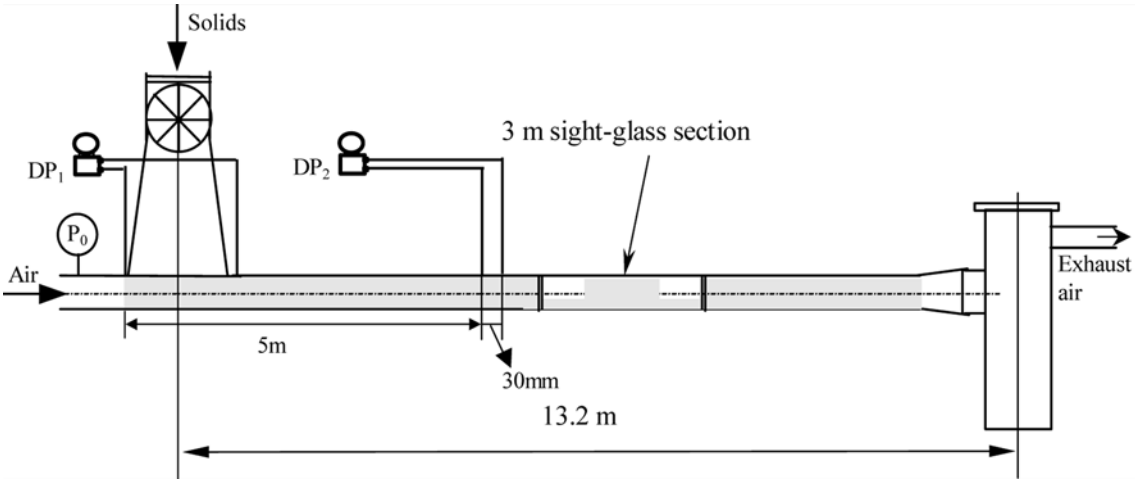

Fig. 1. Schematics of experimental rig

a. when $\varepsilon'_g < 0.8$, using Ergun's equation.

$$F_D = 1/2\pi \mathbf{R}^2 \rho_g C_D \left|\mathbf{u}-\mathbf{v}\right| (\mathbf{u}-\mathbf{v}) \tag{12}$$

$$C_D = \varepsilon_g'^{-1}\left(\frac{200\left(1-\varepsilon'_g\right)}{\mathrm{Re}}+\frac{7}{3}\right)$$

b. when $\varepsilon'_g > 0.8$, using Wen and Yu's expression.

$$F_D = 1/2\pi \mathbf{R}^2 \rho_g C'_D \left|\mathbf{u}-\mathbf{v}\right| (\mathbf{u}-\mathbf{v}) \tag{13}$$

$$C'_D = C_D \varepsilon_g'^{-2.65}$$

$$C_D = \begin{cases} \frac{24}{\mathrm{Re}}(1+0.15\mathrm{Re}^{0.687}) & ,(\mathrm{Re}<1000) \\ 0.44 & ,(\mathrm{Re}\geq 1000) \end{cases}$$

$$\mathrm{Re} = \frac{\rho_g \varepsilon'_g d_p \left|\mathbf{u}-\mathbf{v}\right|}{\mu_g}$$

where d_p the particle diameter, C_D the drag coefficient for an isolated particle, C'_D the modified drag coefficient,$\mathbf{v}$ is the average velocity of particles in the cell.

For gas phase, the total drag force by the particles in the cell is shown below,

$$F_{t,D} = \sum_{i=1}^{n} F_D / V_{cell}$$

V_{cell} is the volume of the cell.

3 Experimental verification of the model

Experimental work was undertaken in order to verify the model. Figure 1 shows the experimental equipment, which includes a feeder hopper, a receiving hopper, and a single ended pressure transducer, and two differential pressure transducers. The transducers provided the information about plug formation and development.

The physical properties of particles (Coefficient of friction, Poisson ratio, coefficient of restitution) are standard values found in the literature. As Tsuji et al. [3] demonstrated that assuming a smaller value for the particle stiffness can still produce realistic particle motion while reducing the computation time, the value of Young's modulus is smaller than the realistic value and reduced by 30 times. The value is verified by the Energy dissipation system.

Table 1. Conditions of Plug Flow

Pipe and flow	
Pipe diameter (mm)	80
Pipe length (mm)	8000
Solids flow rate (kg/s)	1.29
Air flow rate (kg/s)	0.0261
SLR	45.4
Superficial air velocity (m/s)	4.26
Gas	
Gas used	air
Density	by ideal gas law
Particles	
Material	Nylon
Shape	Spherical
Maximum particle number	40000
Particle density (kg m^{-3})	1135
Particle diameter (mm)	3
Coefficient of friction	0.3
Poisson ratio	0.33
Coefficient of restitution	0.8
Young's modulus (Pa)	3E+7

4 Results and discussions

Figure 2 shows the formation and motion of the dune. For the first few seconds, particles pile up at the bottom of the pipeline and form a dune. When the dune reaches the top of pipeline, the air pushes it forward.

Figure 3 shows the phenomena of a plug's collapse. It is clearly observed that at the time 5.2 seconds, the front of plug is at 4.2 m along pipeline, but on the right side of the plug, the pipeline is nearly empty, this plug collapses and forms the stationary layer. These figures agree with actual phenomena observed in the plug of cohesionless particles.

Figure 4 shows the developed plug travel through the pipeline. Due to the previous plug forming the stationary layer, this plug easily moves out the pipeline. It is found that in the front of plug, the particles are loose and faster than other particles and drop down by gravity.

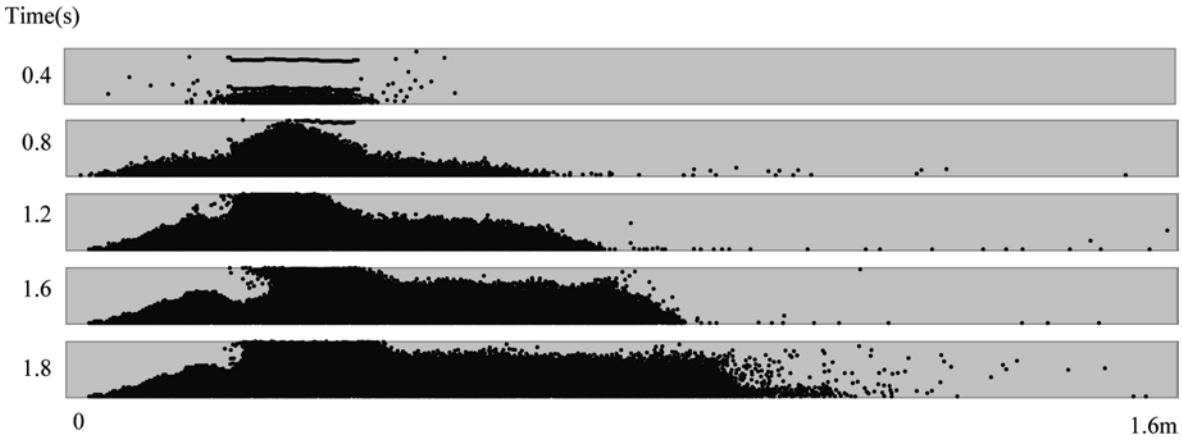

Fig. 2. The formation of plugs simulated by the model

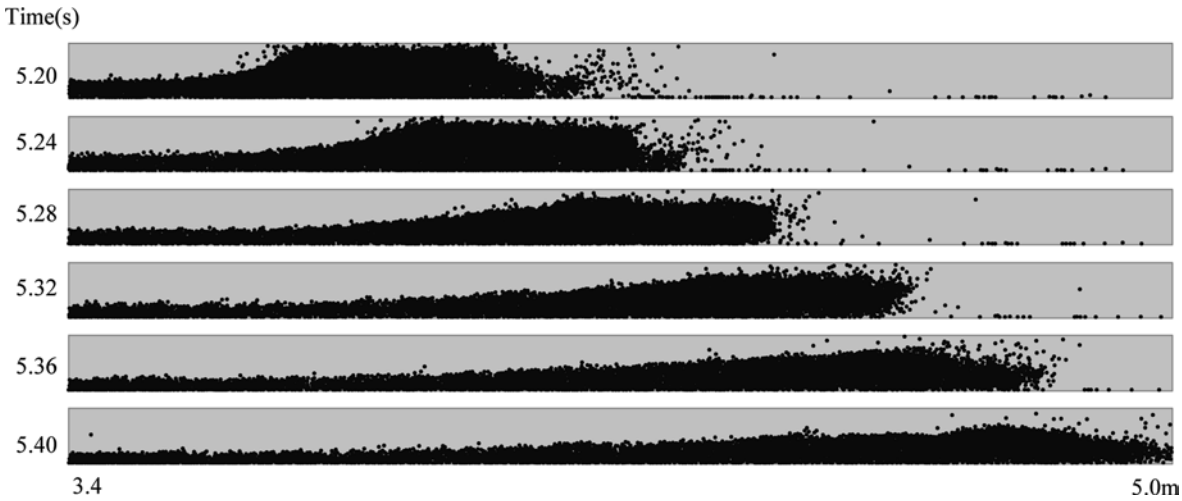

Fig. 3. The collapse of one plug simulated by the model

Fig. 4. Motion of one plug simulated by the model

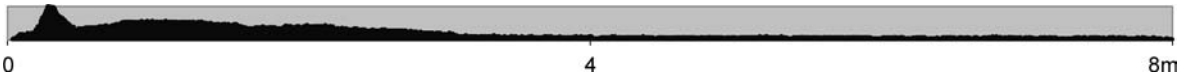

Fig. 5. The stationary layer after conveying simulated by the model

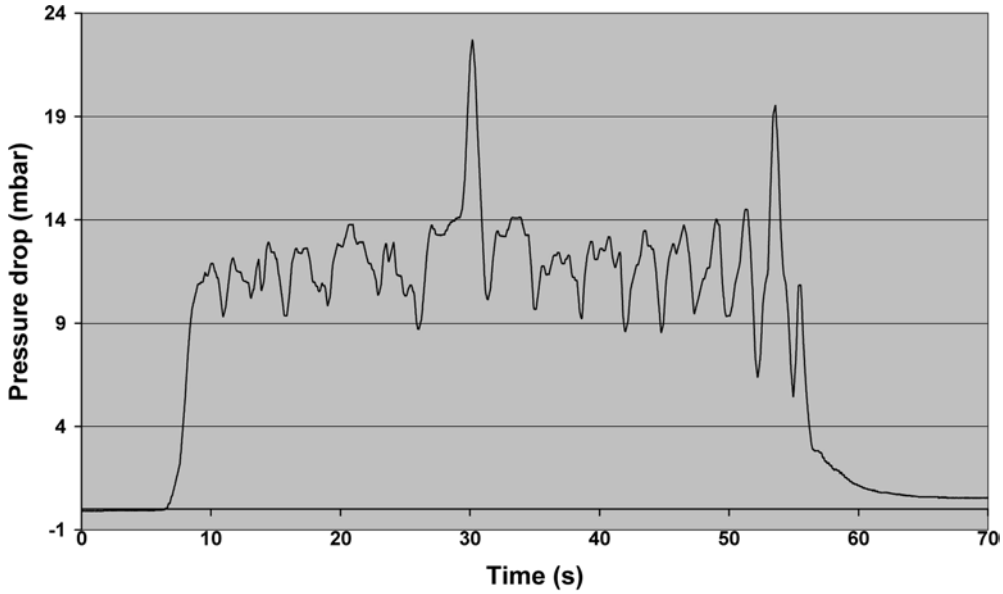

Fig. 6. Recorded pressure trace for DP1 in experimental test

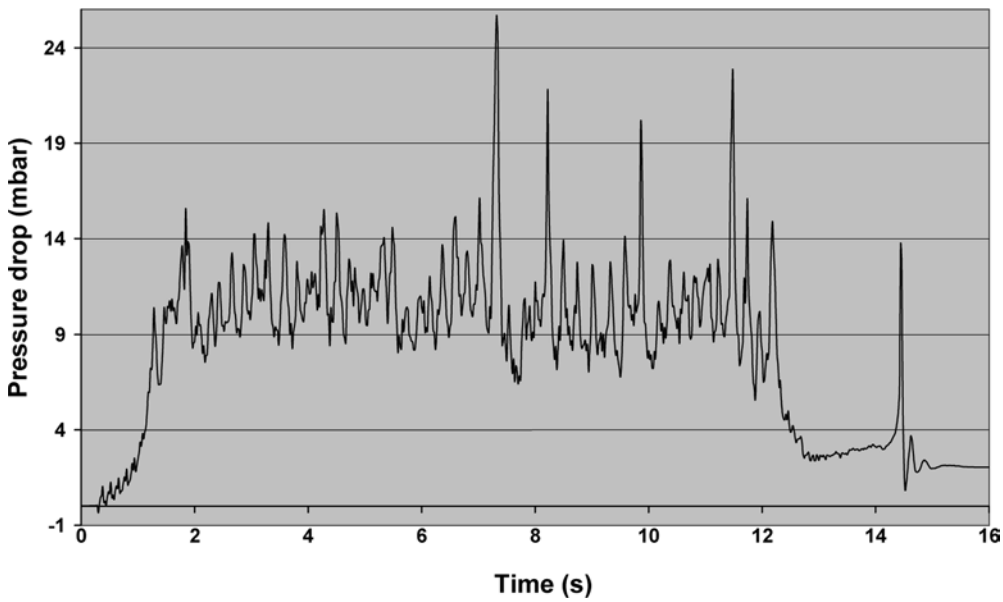

Fig. 7. Recorded pressure trace for DP1 in simulation

Figure 3 and figure 4 also show that in order to form a stable plug, the thickest of the stationary layer should over a certain value.

After 10 seconds, the model stopped inputting particles in the dropout box, mimicking the experiment closure of the feeder valve. Figure 5 shows time at 16 seconds. All plugs have moved out of the pipeline. The stationary layer was left in the pipeline.

The output of transducer DP1 (in Figure 1) is shown in Figure 6 and compared with the model's results shown in figure 7. Because of the limited CPU time, the simulation time is 18 seconds, and the whole process of experiment is 70 seconds. The maximum pressure drop in the simulation is about 25 mbar. After closing valve of the feeder, a peak appears, this is due to the remaining particles forming a plug and moving forward. These model results agree well with the experimental data. In the model values of the minimum pressure drop between two peaks are different from experimental data. The values from the model are above 8 mbar, compared with 9 mbar from experimental results. This difference may be due to the model's virtual transducer's response time being absolute 0 second,

whereas the real transducer response is relatively slow. Another reason is that the model used is a two dimensional model.

5 Conclusions

A gas-solids two-dimensional mathematical model was developed to simulate particle motion in dense phase pneumatic conveying based on a combined approach of the Discrete Element Method (DEM) and Computational Fluid Dynamics (CFD). The results of this model presented in this paper are compared and agree well with experimental test data. It has been found that this model can simulate most of the observed processes as of particle motion in dense phase pneumatic conveying, such as plug formation, plug collapse, and plug movement. As such, it may have a direct application in understanding the process of dense phase flow.

Further work will be carried out to develop a three-dimensional mathematical model and fully simulate the particle motion in dense phase pneumatic conveying.

References

1. K. Konrad, Dense-phase pneumatic conveying: a review, Powder Technology 49 (1986), p. 1–35
2. P. A. Cundall & O. D. L. Strack, A discrete numerical model for granular assemblies, G'eotechnique 29 (1979), p. 47–65
3. Y. Tsuji & T. Kawaguchi & T. Tanaka, Discrete particle simulation of two-dimensional fluidized bed, Powder Technology 77 (1993), p. 79–87
4. Y. Tsuji, Lagrangian numerical simulation of plug flow of cohesionless particles in a horizontal pipe, Powder Technology 71 (1992), p. 239–250
5. D. Zhang & W. J. Whiten, The calculation of contact forces between particles using spring and damping models, Powder Technology 88 (1996), p. 59–64
6. S. Ergun, Fluid flow through packed columns, Chem. Eng. Prog. 48 (1952), p. 89–94
7. C. Y. Wen & Y.H. Yu, Mechanics of fluidization, Chem Eng. Prog. Symp. Series. 62 (1966), p. 100–111
8. R. D. Mindkin & H. Deresiewicz, Elastic spheres in contact under varying oblique forces, Journal of applied mechanics 20 (1953), p. 327–344